Application for beam time at GSI/FAIR (continuation request)

mCBM@SIS18 2023/24

A CBM full system test-setup
for high-rate nucleus-nucleus collisions
at GSI / FAIR

The CBM Collaboration

corresponding authors:
Norbert Herrmann and Christian Sturm

Submitted to the
General Program Advisory Committee (G-PAC) of GSI / FAIR
June 30th, 2022

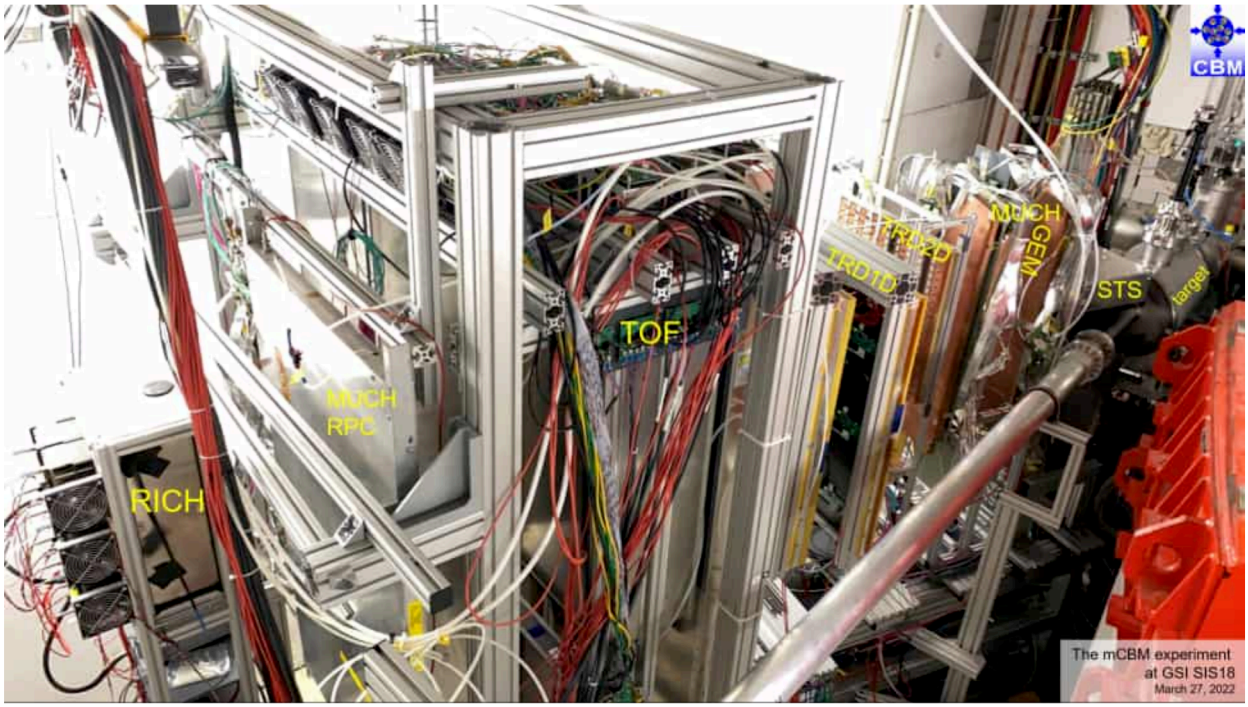

mCBM@SIS18 2023/24 - Application for beam time at GSI/FAIR
Submitted to the General Program Advisory Committee (G-PAC) of GSI / FAIR
on June 30th, 2022

Authors: The CBM Collaboration
Responsible Editors: Norbert Herrmann and Christian Sturm

Publication year: 2025
Publisher: GSI Helmholtzzentrum für Schwerionenforschung GmbH
Planckstraße 1 / 64291 Darmstadt / Germany
License: CCBY4

DOI:10.15120/GSI-2025-00774

Executive summary

This beam time application submitted in June 2022 is a continuation request by the CBM Collaboration to the General Program Advisory Committee (G-PAC) of GSI/FAIR, following the proposals which were granted in 2017 [4] and 2020 [5] within the FAIR phase-0 program of GSI / FAIR. The primary aim of *mCBM@SIS18* (short "mCBM") is to commission and optimize the complex interplay of the different detector systems with the triggerless-streaming data acquisition and the fast online event reconstruction and selection under realistic experiment conditions up to the top CBM interaction rate of 10 MHz. To validate the read-out and data processing concept of CBM the Λ production yield in Au + Au and Ni + Ni collisions at top SIS18 energies are measured with mCBM as a benchmark observable, which will allow comparison with published data by the FOPI and HADES experiment.

During the mCBM beam campaigns 2021 and 2022 systematic high-rate studies could be performed for various detector subsystems in nucleus-nucleus collisions with up to 10 MHz collision rate benefiting substantially from high beam intensities available at the SIS18 of GSI / FAIR. In 2021 major effort was put on the upgrade of the DAQ / data transport system to the final CBM configuration integrating the new Common Readout Interface (CRI). The FPGA firmware for each detector subsystem as well as a new Timing and Fast Control system (TFC) has been newly developed and successfully tested. Hence, a first commissioning run for the benchmark measurements could be taken in O + Ni collisions at 2.0 AGeV kinetic projectile energy in July 2021, followed by the first benchmark runs in May and June 2022 measuring $5{\cdot}10^9$ Ni + Ni collisions at 1.93 AGeV and $2{\cdot}10^{10}$ Au + Au at 1.23 AGeV.

For the years 2023 and 2024, we apply to continue the mCBM project as an ideal test bed for commissioning and optimizing the triggerless-streaming data transport and the online / offline software packages under realistic experiment conditions. Thus, we apply for 6 shifts as secondary user for each year, performing high-rate studies on the CBM detector systems and the CBM triggerless-streaming DAQ and data transport with mCBM at SIS18.

We apply to expand the benchmark measurements on sub-threshold Λ production with mCBM at SIS18, performing energy scans down to low incident energies. There, Λ production becomes extremely rare, benefiting most from the extreme rate capability of the CBM systems, especially the online reconstruction and selection. We expect that these runs will produce new data, to be published in peer-reviewed journals. For this program we apply for 18 shifts as main user, in addition a commissioning block with 3 shifts as secondary user for each year 2023 and 2024.

In continuation of the successful CBM MVD program at the UNILAC we apply to test the next generation Monolithic-Active-Pixel-Sensor (MAPS) prototype MIMOSIS-2 with UNILAC beam at the M3 and μX0 facilities. We hence apply as main user for 12 shifts at the M3 and 6 shifts at the μX0 facility for 2023 and 2024 each.

1 Achievements of the mCBM beam campaign 2021

1.1 Setup

The mCBM experiment was set up in 2017 and 2018 at the detector test area HTD situated at the beam entrance of the experimental area Cave-C (HTC), hosting the nuclear structure experiment R^3B. As depicted in Figure 1.1.1, the mCBM experiment is positioned downstream a solid target under a polar angle of about 25° with respect to the primary beam towards a beam dump located 7 m downstream at the south end of the experimental area. mCBM does not comprise a magnetic field, and measures therefore charged particles produced in nucleus-nucleus collisions traversing the detector stations under straight trajectories. The mCBM setup includes currently detector stations of all CBM subsystems. For the 2021 campaign the GEM stations for the MUCH system could not be upgraded due to pandemic travel restrictions and hence, the MUCH detector was not mounted. Figure 1.1.1 depicts the top view of the GEANT geometry of the the mCBM 2021 setup.

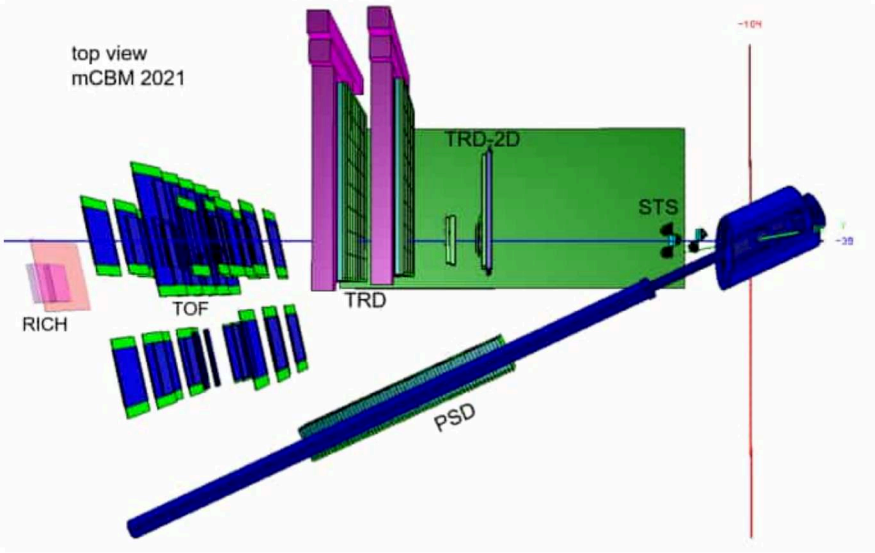

Figure 1.1.1: The mCBM setup as of June 2021 in GEANT. The beam enters from the right.

As visible in Figure 1.1.1 the mCBM experiment for the 2021 beam campaign comprised of:

- the Silicon Tracking System (STS) subsystem which was fully equipped with 2 stations, 5 STS ladders in total,
- two large Transition Radiation Detector (TRD) stations which were complemented with two detectors for the inner TRD region (TRD-2D),
- the Time-of-Flight (TOF) subsystem consisting of 6 modules was grouped into two stacks; the TOF mainframe was moved and rotated closer to the optical beam axis positioning the inner stack at a center polar emission angle of 12.5° and the outer stack at 25.0°; RPC counters under test were placed for high-rate studies in between the TOF modules of the inner stack,
- the Ring Imaging Cherenkov (RICH) subsystem using two aerogel radiators was placed directly behind the TOF detector and delivers a second measurement of the particle velocity in a selected acceptance window,
- a single Projectile Spectator Detector (PSD) prototype-module positioned directly under the optical axis of the beam, 5° tilted relative to the beam axis while pointing to the target.

Furthermore, the vacuum system of the mCBM experiment has been completed with an Aluminum beam pipe. The fast and segmented diamond counter for time-zero (T0) determination positioned 20 cm upstream of the target has been used during the high-rate tests using the former AFCK-based data transport (see details in [5]), but could not be included into the new CRI-based data transport (see section 1.2).

For high-rate studies in nucleus-nucleus collisions the TOF mainframe was moved and rotated towards smaller polar emission angles, significantly enhancing the charged particle rate observed at the inner TOF stack. Hence, RPC counters under test were placed in between the TOF modules of the inner TOF stack. Furthermore, MIMOSIS-I sensors for the Micro Vertex Detector (MVD), LGAD sensors for the beam monitoring system as well as STS front-end electronics were placed for radiation hardness studies in front of the SEM-grid beam counter, upstream of the mCBM beamdump, directly on the beam axis (not visible in Figure 1.1.1).

The DAQ/data transport as well as the detector subsystems were remotely controlled by VNCs while the communication was provided by permanent Zoom rooms. During shifts, the mCBM experiment could thus be operated properly with a small team of 4 to 6 persons on-site and about 20 experts word-wide connected remotely.

1.2 Data acquisition and data transport

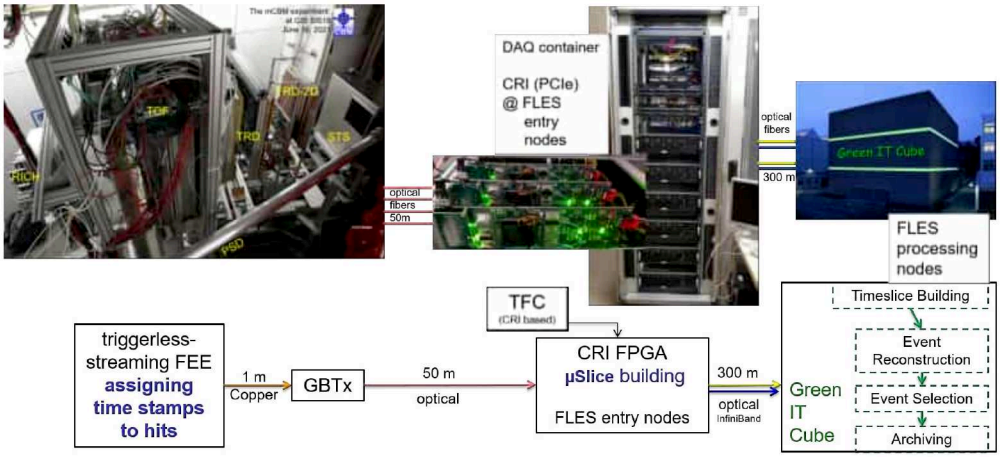

Figure 1.2.1: The CBM DAQ and data transport system based on CRIs, applied to mCBM.

The CBM experiment at FAIR will measure relativistic nucleus-nucleus collisions with collision rates up to 10 MHz leading to data rates up to 1 TB per second. To achieve the required performance a triggerless-streaming data acquisition system is being developed. For the mCBM beam campaign 2021 the major effort was put on the upgrade of the DAQ system to the final CBM configuration by merging two FPGA layers (DPB and FLIB, see [5]) into a Common Readout Interface (CRI) [6].

The CBM DAQ and data transport system as it is used in the mCBM setup is depicted in Fig. 1.2.1. It includes ultra-fast and radiation-tolerant ASICs as front-end chips followed by CERN GBTx-based radiation-tolerant data aggregation units. The detector front-end digitizes signals above threshold and assigns a time stamp to the hit. By means of a Timing and Fast Control (TFC) system the detector front-ends are time-synchronized to the nanosecond level. This data is then forwarded via an electrical connection to the GBTx readout board, where the electrical signals acquired through a large number of e-links are converted and merged into an optical GBT link operating at a link speed of 4.48 Gbit/s. These GBT links interface the detector subsystems with the PCIe-based CRI boards integrated in the First Level Event Selector (FLES) input nodes. The present CRI version (v1.0, "BNL-712 v2") has been developed by the Brookhaven National Laboratory (BNL) and is based on the XILINX Kintex UltraScale FPGA. The required, new FPGA firmware [14] has been developed in Q3.2020 - Q2.2021 for each detector subsystem as well as for the TFC system [17],[16]. Merging of two FPGA layers (DPB and FLIB) into a single FPGA CRI board required the development of a new FLES Interface Module (FLIM) [15]. Furthermore, a scalable Experiment Control System (ECS) has been embedded in the upgraded DAQ and data transport system.

1.3 Results

High-rate studies

During the mCBM campaign 2021 various beams could be used to perform high-rate studies in nucleus-nucleus collisions with collision rates up to 10 MHz benefiting substantially from the highest available beam intensities. The used ion species with the corresponding kinetic project energies T_{proj} as well as highest beam intensities are listed in Table 1.3.1. Hence, systematic high-rate studies could be performed investigating the TOF RPC rate capability at the highest collision rates, the bit-flip and latch-up probability of the MVD MIMOSIS-I sensor and the front-end ASIC of the STS system (STS-XYTER v2.2). Additionally, first tests on the rate capability of LGAD sensors potentially suited for the CBM beam monitor system could be conducted. First results indicate a remarkable radiation tolerance of all tested components.

2021	projectile	T_{proj}	max. beam intensity per spill (10s)
March	^{208}Pb(67+)	1.06 AGeV	$2{\cdot}10^9$
May	^{124}Xe(46+)	1.30 AGeV	$3{\cdot}10^9$
June	^{16}O(8+)	2.00 AGeV	$1{\cdot}10^{10}$

Table 1.3.1: mCBM high-rate studies in 2021.

Fig. 1.3.1 shows the TOF RPC efficiency (left figure) and the time resolution of the RPCs (right figure) as a function of the observed counting rate [12]. The efficiency degrades only slightly with the counting rate. The time resolution reduces to the measured 70 ps for the system and 52 ps for single counters at the highest counting rates of about 25 kHz/cm^2 showing a sound performance, well in line with the requirements of the CBM TOF system. It is worth mentioning that the time distribution remains Gaussian shape at the highest counting rates.

The first full-sized sensor prototype MIMOSIS-1 for the MVD was placed in front of the mCBM beam dump, being directly exposed by the ion beam under various beam intensities, operated in ~ 1 AGeV Xe and Pb-beams. The tests were performed to simulate the beam halo during CBM experiments at the SIS100 [7]. Hence, the sensor was tested for two Single Event Effects (SEE): Bit flips (BF), which may corrupt data in particular in the status registers of the sensor and Single Event Latchups (LU), which create short circuits in the device and destroy it thermally unless they are extinguished by a power cycle in time. BF were spotted by reading back the content of the resisters, LUs by detecting the related over-currents in the biasing lines. The experiment showed that BFs and LUs could not be rigorously distinguished as some BF modified the sensor operation mode such that additional currents similar to a LU signature were consumed. An overall SEE cross-section of $\lesssim 10^{-7}$ cm^2 was found for the Au-beam (preliminary upper limit), which is considered as satisfactory. The unexpectedly high rate of BFs was associated to a bug in the protection circuits of the related registers, which was fixed for the follow-up sensor MIMOSIS-2.

Similar to the MVD MIMOSIS-1 sensor tests, the front-end ASIC of the STS system STS-XYTER v2.2, mounted on a front-end board, was exposed by direct Pb beam with different beam intensities while placed in front of the mCBM beam dump [8]. With beam intensities up to 10^7 Pb ions per second on the ASIC no Latch-Up Transitions (LUTs) were observed. At higher beam intensities the LUT related current increased, and at the highest beam intensities LUTs became frequent, but without showing severe damages. Power cycling returned the measured current to the original value. With the estimated LUT probability of of approx. $6{\cdot}10^{-10}$ per Pb-ion no major risk is expected for the operation of the CBM STS since the front-end boards with mounted ASICs will be positioned outside the detector acceptance with large distance to the primary beam.

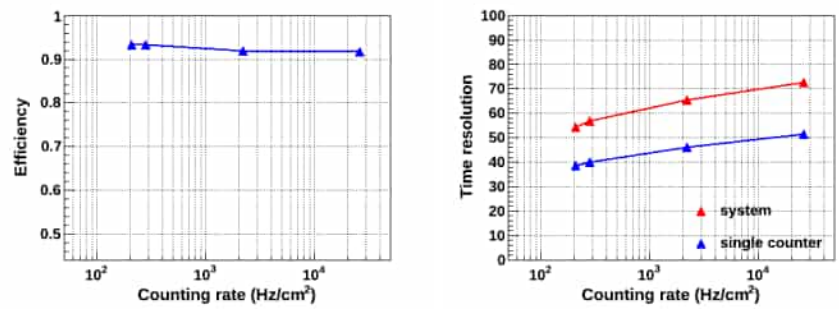

Figure 1.3.1: Left panel: TOF RPC efficiency (HV: +/-6 kV, 200 mV FEE threshold) and time resolution as a function of the charged particle flux (right figure), see [12].

Furthermore, permanent damages by LUTs could not be observed and can be circumvented if detected fast enough.

Commissioning run for the benchmark measurements in 2022

The new DAQ hardware and 1^{st} firm- and software versions for the new DAQ system and data transport were successfully tested during the ^{16}O-beam block in July 2021. O + Ni collisions at 2.0 AGeV kinetic bombarding energy were measured with max. 1 MHz collision rate as a first commissioning run (# 1588) for the planned benchmark campaign on Λ production in 2022. As a key requirement of a triggerless-streaming DAQ system, the CRI branches of all detector subsystems were stably synchronized over the full run period. Hence, a stable timing of the front-end electronics of all detector subsystems could be observed within the expected time resolution as it is visible in Figure 1.3.2. Here, all time differences $time\ diff\ =\ (t_{subsystem} - t_{TOF})$ are displayed within the given time window measured by the STS, TRD, PSD and RICH detector subsystes with respect to the time of the TOF system. The measured time results from time stamps assigned to the raw hit messages by their front-end ASICs, converted into digis with unit [ns] during the unpacking stage of the data analysis. Individual time offsets of the subsystems are corrected during the unpacking stage, no detailed time calibration procedures were applied. As observed, the subsystem time offsets remain constant during the run as well as between runs. Supplementary to the correlation in time, correlations of spatial coordinates are presented in Fig. 1.3.3 [9], exemplary between both STS stations STS 0 and STS 1 (left figure) and between STS stations and TOF modules (right figure).

First data-driven alignment studies have been performed correcting the position of the STS stations with respect to the target [9] as well as of TOF with respect to STS and target [13]. Both are based on forming tracklets projecting to the target, either using both STS stations [9] or in a row of stacked modules of the TOF wall involving the position of the STS units [13]. While doing so, the reconstruction of the vertex turned out to be a suitable tool, being sensitive to x and y as well as z-shifts of the detector units and stations. The resulting vertex reconstruction is shown in Fig. 1.3.4. The dimension of the reconstructed vertex matches reasonably with the beam spot measured on the scintillation target of the beam diagnostics station, upstream in front of the mCBM target chamber.

A preliminary CBM data analysis chain is being developed. As a first step, the raw data messages packed and compressed in TimeSliceArchive (tsa) files are being unpacked by an unified unpacking scheme separating the framework from the algorithmic part [18]. Accordingly, the subsystem-specific unpacking converts the raw data messages into CbmDigiEvents (Digi classes) within this common architecture, applying additionally individual subsystem time-offset corrections as well as involving the detector channel mapping and (partially) first calibration steps of the corresponding detector subsystem.

After data unpacking, a first, simplified event building is performed based on a time-cluster-search within a time window defined by the timing response of a reference detector system [19]. The digi-times of the reference detector are then taken as seeds for setting the time windows of the detector systems by adapting the window width according to the corresponding timing response. The identified event candidates are further filtered by digi-based trigger conditions [20], [21] cutting e.g. on digi-multiplicities of selected detector stations or it's combinations. For mCBM data taken during the benchmark commissioning run O + Ni at 2.0 AGeV in July 2021 the trigger condition of the event candidate selection requests $M_{TOF\ \mathrm{digi}} \geq 6$.

Subsequently, detector hits are reconstructed by the subsystem specific hit finding algorithms applied to digi events. Reconstructed hits have been used for spatial correlations shown in Fig. 1.3.3 as well as for the vertex reconstruction displayed in Fig. 1.3.4. Furthermore, TOF tracklets are formed based on reconstructed TOF hits using both active layer of the TOF configuration included into the new CRI readout in July 2021. TOF tracklets have been used e.g. to project onto the STS detector planes towards the target for efficiency studies of the STS [9] or for investigations on the alignment of detector stations [13]. The well-developed and investigated CBM track

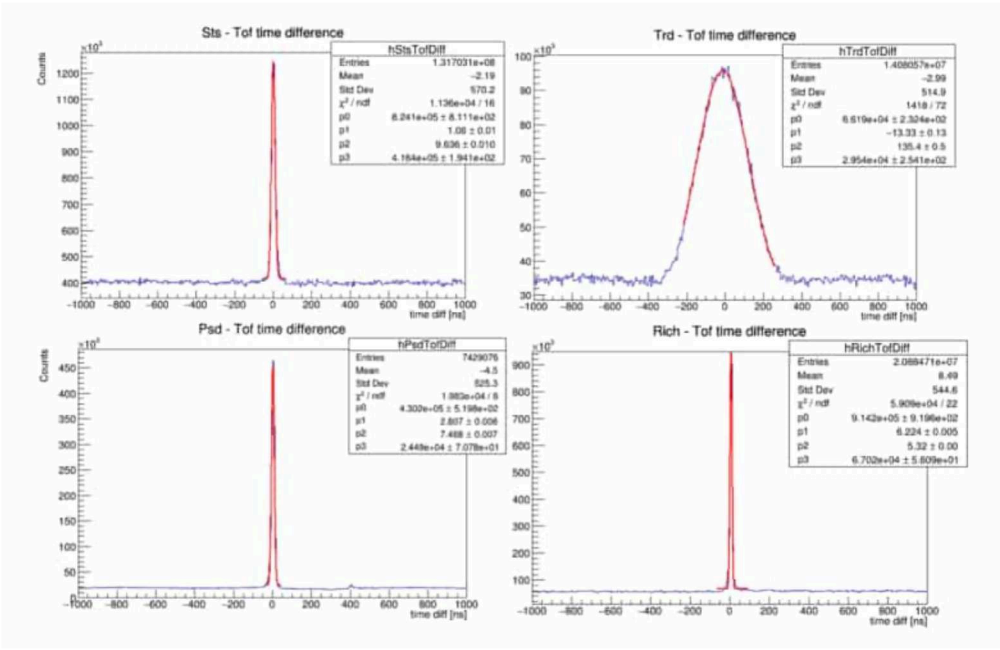

Figure 1.3.2: Stable timing: time difference measured by the detector subsystems with respect to the TOF system.

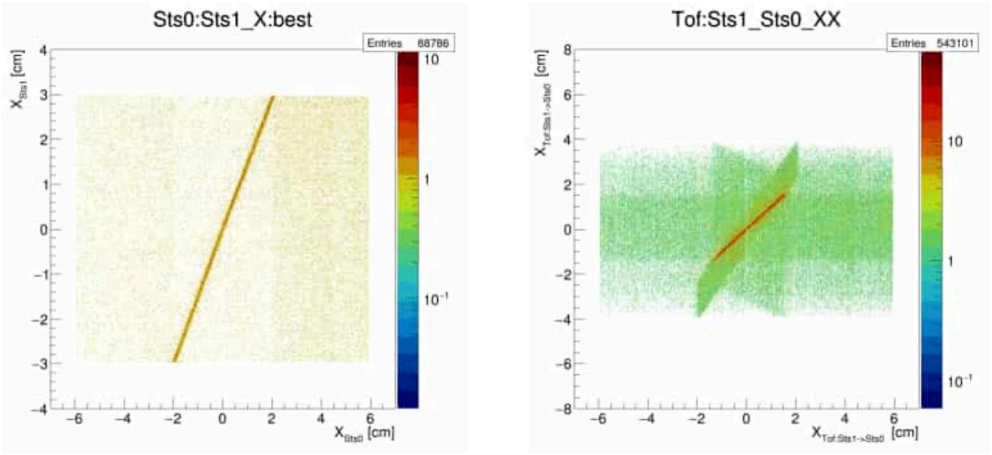

Figure 1.3.3: Correlation between spatial coordinates (x) of both STS stations STS 0 and STS 1 (left figure) and between both STS stations and TOF (right figure) [9].

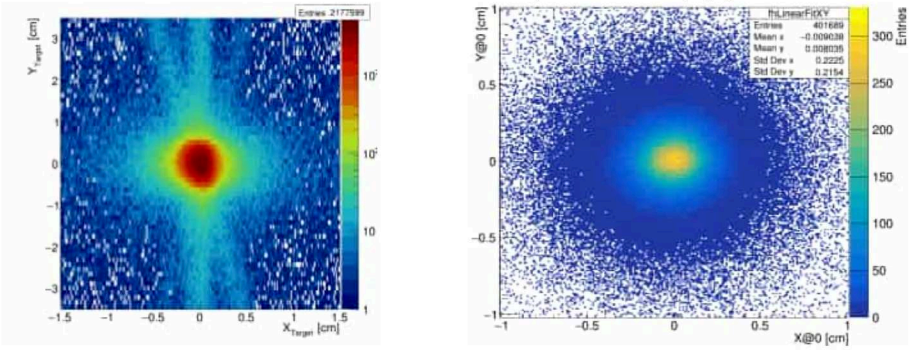

Figure 1.3.4: Vertex reconstruction after a first alignment by correcting the position of the STS stations with respect to the target [9] (left figure) as well as of TOF with respect to STS and target [13] (right figure).

reconstruction algorithm *Cellular Automaton Tracking* (CA) has been adapted for application on mCBM simulations and experiment data [22]. Moreover, the flexibility of the track reconstruction approach could be expanded significantly by a standardized interface. Hence, the CA tracker can be applied soon to real mCBM data, enhancing the selection power especially for heavy collision systems, which were measured during the beam campaign 2022. Although the acceptance of the STS, TRD2D and TOF detector systems was limited in 2021, Monte-Carlo simulations showed the feasibility for Λ reconstruction with the 2021 setup. However, the absolute time-of-flight calibration and hence the reconstruction failed since the T0 diamond counter was not yet included into the newly established CRI data transport (see chapter 1.1).

2 The beam campaign 2022

The intensive preparation phase for the beam campaign 2022 started with first dry runs in December 2021. Cosmics runs were added in January 2022 studying detector response and system timing as well as testing a first online selection based on correlated hits within detector system-specific time windows. First commissioning with beam was conducted in March 2022 taking a few hours ^{12}C(6+) beam at 2.0 AGeV and ^{56}Fe(26+) at 1.8 AGeV. High-rate studies were performed especially for the TOF and MUCH detector systems with ^{238}U(73+) at 1.0 AGeV beam end of March and with ^{197}Au(67+) at 1.13 AGeV in June 2022.

Prior to the benchmark runs in May and June 2022 enhancing the capability of the mCBM setup, additional front-end boards were installed on the TRD2D detector system expanding the read-out area significantly. Furthermore, a new T0 diamond counter was mounted with $1\times1\,\mathrm{cm}^2$ area partitioned in 16 strips on both sides, vertically and horizontally aligned (the read-out of the horizontal strips will be added for the 2023 campaign). On May 26, 2022, the first benchmark run has been measured taking Ni + Ni collisions at 1.93 AGeV kinetic projectile energy T_{proj}. With a total run duration of 5 h 55 min approx. $5{\cdot}10^9$ collisions were collected on 30 TB tsa files storing the raw data messages. The second benchmark run was taken on June 16 - 18, 2022, measuring Au + Au collisions at 1.23 AGeV with a total run duration of 34 h 33 min collecting approx. $2{\cdot}10^{10}$ collisions on 180 TB tsa files. Table 2.0.1 summarizes the mCBM data taking in 2022. Although an online selection based on the unpacked, time-offset corrected subsystem data was technically feasible raw data were completely archived in order to minimize the risk of uncontrolled data losses. Data analysis steps like calibrations and detector alignment for the benchmark runs as well as for the detector high-rate studies are ongoing.

2022	Projectile	T_{proj}	Beam intensity per spill (10s)	Av. collision rate	Objective
March 29 - April 1	^{238}U(73+)	1.00 AGeV	10^7 - 10^9	100 kHz - 10 MHz	high-rate studies TOF & MUCH
May 26	^{58}Ni(28+)	1.93 AGeV	$4{\cdot}10^7$	400 kHz	benchmark run I
June 16 - 18	^{197}Au(69+)	1.23 AGeV	2 - $3{\cdot}10^7$	200 - 300 kHz	benchmark run II
June 19 - 20	^{197}Au(67+)	1.13 AGeV	$1{\cdot}10^7$ - $4{\cdot}10^8$	100 kHz - 4 MHz	high-rate studies TOF & MUCH

Table 2.0.1: mCBM data taking in 2022.

MVD tests at the UNILAC

The Single Event Effect (SEE) tests with MIMOSIS-1 carried out with the ~ 1 AGeV heavy ion beams at SIS18 in 2021 were complemented with a test campaign at the M3 and X0-beam line

at UNILAC in 2022. The M3 beam tests provided valuable additional information thanks to the by far superior dosimetry and the option to define regions of interest by means of masking the ~ 5 AMeV Ca beam. No LUs were observed for this 20 MeV $\cdot$ cm^2/mg beam up to an exposure of few 10^{10} ions/cm^2. The signatures interpreted as LUs at mCBM were reproduced by provoking BFs in the registers steering the on-chip DACs. The sensors tolerated ion fluences expected for direct SIS100 beam impact into the MVD without major loss of functionality. If confirmed by the ongoing analysis and the proposed follow-up tests, those results may allow to relax the so far harsh requirements on the beam stop system for CBM and the LV-system of the CBM-MVD. Test on the X0-beam line aimed for locating the sources of bit flips. The data collected is currently being analyzed.

3 Requirement on beam time

The beam time application for the years 2023 and 2024 of the mCBM experiment at SIS18 is summarized in Table 3.1.2, subdivided into lines (1) - (6), and for CBM MVD tests at the UNILAC in Table 3.2.1, lines (7) - (10).

3.1 mCBM at the SIS18

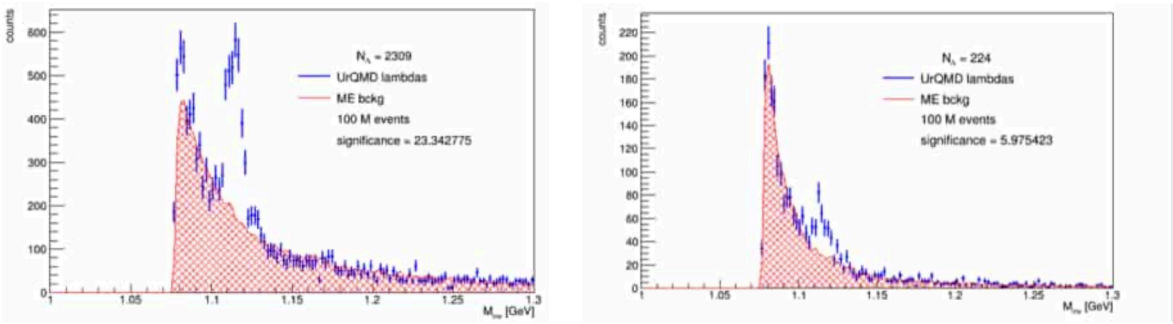

Figure 3.1.1: Monte-Carlo Simulations on Λ reconstruction with mCBM: the invariant mass distributions are obtained in 100M minimum-bias Ni + Ni collisions at 1.93 AGeV (left figure) and Au + Au at 1.24 AGeV (right figure) - (event-based simulations, event generator: UrQMD, mCBM setup 2022_04).

Following successful high-rate studies during the mCBM beam campaigns in 2021 and 2022, additional systematic studies at high and highest available beam intensities need to be performed. We therefore apply (1) + (4) for 6 shifts each year as secondary user to further investigate the rate capability and response of the detector subsystems, potential aging effects and the performance of the triggerless-streaming DAQ and data transport system at high and highest loads.

Results on Λ production in Ni + Ni collisions at 1.93 AGeV has been published by the FOPI collaboration [2] and in Au + Au collisions at 1.24 AGeV by the HADES collaboration [1]. Furthermore, the HADES experiment has taken data on Ag + Ag collisions at 1.58 AGeV in March 2019, first results on Λ production are expected soon. Hence, Au + Au, Ag + Ag and Ni + Ni collisions at top SIS18 projectile energies are well suited to benchmark the CBM triggerless-streaming DAQ systems including firm- and software as well as the online/offline software packages with mCBM. We thus apply to continue with benchmark (physics) runs at mCBM in the years 2023 and 2024, laying emphasis on the online/offline Λ reconstruction in Ni + Ni and Ag + Ag and collisions.

Since mCBM does not include a magnetic field for momentum measurement, Λ reconstruction has to be done via time-of-flight (TOF) and track topology. The reconstruction scheme as well as the used topological cuts have been described within the initial mCBM proposal [4]. Applying the reconstruction scheme to Monte-Carlo simulations using the mCBM 2023 setup results to the invariant mass distributions shown in Fig. 3.1.1 demonstrating that the limited information

Collision system	M_Λ, reconstr.	Av. collision rate	Beam intensity per spill (10s)	N_Λ reconstr. per 8h-shift
Ni + Ni 1.93 AGeV	$2.3{\cdot}10^{-5}$	400 kHz	$4{\cdot}10^{7}$	90k
Au + Au 1.24 AGeV	$2.2{\cdot}10^{-6}$	200 kHz	$2{\cdot}10^{7}$	4.4k
Ag + Ag 1.58 AGeV	$5{\cdot}10^{-6}$	300 kHz	$3{\cdot}10^{7}$	15k

Table 3.1.1: Rate estimate for Λ reconstruction with mCBM: the Λ yields for Ni + Ni collisions at 1.93 AGeV and for Au + Au at 1.24 AGeV are taken from simulations depicted in Fig. 3.1.1. Yields for Ag + Ag collisions at 1.58 AGeV were interpolated from above listed Ni and Au simulations (median in mass number and kinetic projectile energy). With a spill length of 10 s, 4 spills per minute and a duty cycle of about 0.5, approx. 1000 spills are taken per 8h-shift. The benchmark runs will be measured at moderate beam intensities resulting to 200 - 400 kHz averaged collision rate while using 10 % interaction probability targets.

available for Λ reconstruction is sufficient. As displayed, the Λ yield drops in Au + Au collisions by a factor of about 10 due to the reduced kinetic projectile energy of 1.24 AGeV which is well below the production threshold in binary nucleon-nucleon collisions causing Λ production to become even more rare. To safely identify the Λ signal in Au + Au collisions the TRD stations were included into the (simplified) track reconstruction. Furthermore, the cuts were optimized with the TMVA machine learning method implemented in the ROOT software package. Both enhances signal-to-background significantly. The simulation results shown in Fig. 3.1.1 are used to estimate Λ yields measured with mCBM in Ni + Ni collisions at 1.93 AGeV and Au + Au at 1.24 AGeV as well as interpolating to Ag + Ag at 1.58 AGeV, as given in Table 3.1.1. For this rate estimate moderate collision rates of 200 - 400 kHz were conservatively assumed.

Estimating Λ yields at lower projectile energies the production excitation function of K^+ mesons predominantly created associated with Λ hyperons is used. The K^+ meson production excitation

	Year	Objective	Projectile	Intensity per spill	Extraction	User type	Shifts
(1)	2023	high-rate detector studies	ions 1 - 2 AGeV, preferably: Au, Pb, U	10^{7} - 10^{9}	slow, 10 s	secondary	6
(2)	2023	commissioning for benchmark run	ions 1 - 2 AGeV, preferably: Ni 1.93 AGeV	10^{7} - 10^{8}	slow, 10 s	secondary	3
(3)	2023	benchmark runs, Λ production excitation function	Ni 1.93, 1.58, 1.23, 1.0 AGeV	10^{8}	slow, 10 s	main	18
(4)	2024	high-rate detector studies	ions 1 - 2 AGeV, preferably: Au, Pb, U	10^{7} - 10^{9}	slow, 10 s	secondary	6
(5)	2024	commissioning for benchmark run	ions 1 - 2 AGeV, preferably: Ag 1.58 AGeV	10^{7} - 10^{8}	slow, 10 s	secondary	3
(6)	2024	benchmark runs, Λ production excitation function	Ag 1.58, 1.23, 1.0 AGeV	10^{8}	slow, 10 s	main	18

Table 3.1.2: Beam time application for the years 2023 and 2024 on SIS18 beam time for mCBM.

function was measured by KaoS at SIS18 / GSI in Au + Au, Ni + Ni and C + C collisions, see [3] and references therein. Applying the published energy scaling in Ni + Ni collisions the production probability around 1 AGeV is reduced by approx. a factor of 20 in comparison to the highest projectile energy of 1.93 AGeV. For the year 2023 we thus apply for 6 and 5 shifts accumulating sufficient statistics at the lowest kinetic projectile energies at 1.0 AGeV and 1.23 AGeV and for 4 and 3 shifts at 1.58 AGeV and 1.93 AGeV, in total 18 shifts, 6 days in one block as main user, listed in line (3) of Table 3.1.2. One preparation shift for each projectile energy is included. Furthermore, we apply (2) for 6 shifts as secondary user to commission the benchmark run, taken as single shifts or as a single block, at least 7 days prior to the benchmark run. To continue the systematic study on Λ production at sub-threshold energies, we apply for 18 shifts as main user to measure the Λ production excitation function in Ag + Ag collisions at the matching projectile energies 1.58 AGeV, 1.23 AGeV and 1.0 AGeV for the year 2024, listed in line (6) of Table 3.1.2, including a 3 shifts commissioning block (5) as secondary user (at least 7 days prior to the benchmark run). Especially the data taking towards low projectile energies will challenge the CBM online selection, since Λ production becomes more and more rare and hence, an enhanced selection power is required providing substantial development potential for the CBM online / offline software packages. We expect new data on sub-threshold Λ production, which can be published in scientific journals.

3.2 MVD sensor studies at the UNILAC

	Year	Objective	Projectile	Beam intensity	User type	Shifts
(7)	2023	Si-sensor (CPS) study at M3	Ca and Au at max. kin. energy	10^7 /s	main	12
(8)	2023	Si-sensor (CPS) study at μX0	heavy ions (e.g. Au, Bi) at max. kin. energy	max.	main	6
(9)	2024	Si-sensor (CPS) study at M3	Ca and Au at max. kin. energy	10^7 /s	main	12
(10)	2024	Si-sensor (CPS) study at μX0	heavy ions (e.g. Au, Bi) at max. kin. energy	max.	main	6

Table 3.2.1: Beam time application on UNILAC beam at M3 and μX0 for 2023 and 2024.

The CBM Micro Vertex Detector (MVD) will be formed from highly granular CMOS Monolithic Active Pixel Sensors (CPS, Si-sensors). To match the requirements on position resolution, radiation hardness and read-out speed a next generation CMOS Monolithic Active Pixel Sensor named MIMOSIS is being developed. For 2023 and 2024, it is proposed to confirm the immunity of MIMOSIS to LUs to higher LETs relying at the M3 beamline and Au beams at μX0 beamline. Moreover, the improved steering registers found in the novel MIMOSIS-2 prototype need to be tested. Additional tests will check if HI-impacts may create issues in the data path, the synchronization of the state machines and the PLL of the sensor. Again the tests must rely on MIMOSIS-2 as many of those blocks were improved. Moreover, the sensor must be operated with full readout chain in the ion beam. The latter is possible at the UNILAC beam lines only as the radiation hard PCBs required for operating MIMOSIS at the mCBM beam do support the data output. A test at the X0 beam line will allow to spot possible weak structures identified at M3 and to eliminate them before submitting the final MIMOSIS-3 sensor. Thus, we apply for 12 shifts as main user at M3 and 6 shifts as main user at μX0 for each year 2023 and 2024, summarized in Table 3.2.1 line (7) - (10). The results will be presented at international workshops and will hence generate a significant visibility beyond CBM within the CPS/MAPS community.

References

[1] J. Adamczewski-Musch et al. (HADES collaboration),
Sub-threshold production of K0s mesons and Lambda hyperons in Au+Au collisions at sqrt(sNN) = 2.4 GeV, Phys. Lett. B793 (2019) 457-463

[2] M. Merschmeyer et al. (FOPI collaboration),
K^0 and Λ production in Ni+Ni collisions near threshold, Phys. Rev. C 76 (2007) 024906

[3] A.Förster et al. (KaoS Collaboration),
Production of K^+ and of K^- Mesons in Heavy-Ion Collisions from 0.6 to 2.0-A-GeV Incident Energy, Phys. Rev. C 75 (2007) 024906

[4] mCBM@SIS18 - A CBM full system test-setup for high-rate nucleus-nucleus collisions at GSI / FAIR GSI-2019-00977, https://repository.gsi.de/record/220072

[5] mCBM@SIS18 2021 / 22 - A CBM full system test-setup for high-rate nucleus-nucleus collisions at GSI / FAIR, Submitted to the G-PAC of GSI / FAIR, June 10^{th}, 2020, https://sf.gsi.de/f/5897b3d11db444e68895/

[6] Wojciech M. Zabołotny, Grzegorz Kasprowicz, Adrian P. Byszuk, David Emschermann, Marek Gumiński, Krzysztof T. Poźniak and Ryszard Romaniuk,
Selection of hardware platform for CBM Common Readout Interface, Proc. SPIE, vol 10445, 2017, ISBN 9781510613546

Published in the CBM Progress Report 2021, uploaded on CBM's webpage https://www.cbm.gsi.de/

[7] B. Arnoldi-Meadows et al., MIMOSIS-1: Studies on Single Event Effects

[8] J. Lehnert et al., Operational studies with the STS-XYTERv2.2 ASIC

[9] D. Ramirez and A. Toia, Performance of the mSTS detector during the mCBM beam campaign 2021

[10] A. Bercuci et al., Steps towards integration of the TRD-2D detection system with the CBM experiment

[11] A. Bercuci et al., Global space-time correlation of the local TRD reconstruction within the mCBM environment

[12] M. Petris et al., In-beam test of the MSMGRPC prototypes for the CBM-TOF inner zone in the mCBM eperimental setup

[13] A. Weber, C. Sturm, and C. Höhne, First data driven alignment studies of the mCBM setup

[14] W. Zabolotny et al., FPGA-related development for CBM DAQ

[15] D. Hutter, J. de Cuveland, and V. Lindenstruth, A FLES Interface Module for the CRI

[16] V. Sidorenko, D. Emschermann, W.F.J. Müller, and J. Becker, Improvement of time alignment between hardware and software

[17] V. Sidorenko, M. Guminski, W. Zabolotny, W.F.J. Müller, and J. Becker, Prospects of GBT-FPGA as the TFC core interface

[18] P.-A. Loizeau, P. Raisig, V. Friese, D. Smith, A. Weber, and A. Bercuci, A new unified architecture for unpacking, applied to mCBM data

[19] D. Smith, S. Roy, P.-A. Loizeau, and V. Friese, Event building in CBM

[20] D. Smith, S. Roy, P.-A. Loizeau, and V. Friese, A minimum-bias trigger algorithm based on the digi time distribution

[21] S. Roy, D. Smith, P.-A. Loizeau, V. Friese, D. Emschermann, and C. Sturm, Time-based simulation and event building for mCBM

[22] V. Akishina, S. Gorbunov, and S. Zharko, Cellular Automaton Tracking